Leucascandrolide B, a New 16-Membered, Extensively Methyl-Branched Polyoxygenated Macrolide from the Calcareous Sponge *Leucascandra caveolata* from Northeastern Waters of New Caledonia

by **Michele D'Ambrosio**[a]), **Marco Tatò**[b]), **Gabriella Pocsfalvi**[c]), **Cécile Debitus**[d]), and **Francesco Pietra**[a])[e])*

[a]) Laboratorio di Chimica Bioorganica, Università di Trento, I-38050 Povo-Trento
[b]) *Pharmacia & Upjohn*, I-20014 Nerviano-Milano
[c]) European Mass Spectrometry Facility Centre, Area della Ricerca del C.N.R., via P. Castellino 111, I-80131 Napoli
[d]) ORSTOM, Centre de Nouméa, B.P. A5 Nouméa Cédex, Nouvelle Calédonie
[e]) Centro Linceo Interdisciplinare 'Beniamino Segre', Accademia Nazionale dei Lincei, via della Lungara 10, I-11165 Roma

Dedicated to the memory of *Ennio Ciuffarin*

We report a novel, extensively methyl-branched and polyoxygenated 16-membered macrolide, leucascandrolide B (= (1*R**,5*S**,7*R**,9*S**,13*R**,14*R**,15*R**,11*Z*)-5-[(*E*)-1,4-dimethylhept-5-enyl]-1,7,9-trihydroxy-11,14-dimethyl-3-oxo-4,17-dioxabicyclo[11.3.1]heptadec-11-en-15-yl] carbamate; **2**), isolated from the calcareous sponge *Leucascandra caveolata* BOROJEVIC and KLAUTAU from the northeastern coast of New Caledonia. The NMR structural assignments were corroborated by semisynthetic derivatives of **2**, the functional groups and atom connectivity by derivatives **4**–**6** (obtained by acetylation, oxidation, and elimination-solvation, resp.), and the relative configurations by derivative **7** (obtained by carbonation). The preferred conformation of **2**, centered on a chair-like tetrahydro-2*H*-pyran ring formed by intramolecular acetalization, was derived from molecular mechanics and semiempirical calculations which were in agreement with all NMR data. A dilactone 'dimeric' structure **3**, indistinguishable from **2** on the basis of all above data, was ruled out by tandem MS-MS experiments.

1. Introduction. – We have recently described a doubly *O*-bridged, 18-membered new type of macrolide, leucascandrolide A (**1**), which showed high cytotoxicity against human KB tumor cell lines and potent antifungal activity. It was isolated from the calcareous sponge *Leucascandra caveolata* BOROJEVIC and KLAUTAU from the northeastern coast of New Caledonia [1]. This was the first described macrolide – and potently biologically active metabolite – from a calcareous sponge. We have now isolated from the same sponge sample a 16-membered macrolide, leucascandrolide B (**2**), which shares no structural similarity with **1** according to its spectral analysis and its derivatizations.

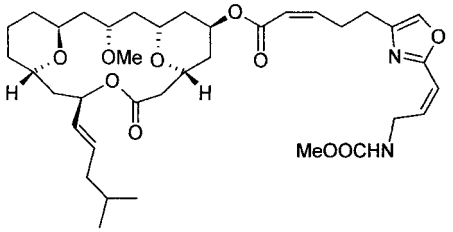

1

2. Results and Discussion. – The minimum C and H count from NMR spectra of leucascandrolide B (**2**), $C_{27}H_{45}$, agreed with a MALDI-TOF-, LSI-, and ESI-MS derived quasi-molecular ion at *m/z* 534 ($[M+Na]^+$), for which probe accurate measurement gave the elemental composition $C_{27}H_{45}NO_8Na^+$. However, in the higher mass range, also ions *m/z* 1023 and 1045 appeared, corresponding to the 'dimeric' ions $[C_{54}H_{90}N_2O_{16}H]^+$ and $[C_{54}H_{90}N_2O_{16}^+Na^+]$, respectively. The intensities of these signals relative to the monomer signal depended on the ionization technique used. 'Dimeric' signals were prominent under ESI conditions (relative intensity of monomer/dimer = 1:3), less prominent in the LSI spectrum (2:1), and only a few percent in MALDI experiments. This was quite intriguing since the NMR data for leucascandrolide B could be interpreted, as shown later, to fit either the monomeric structure **2** or the 'dimeric' structure **3** (see *Scheme*). Collision-induced dissociation (CID) tandem MS (MS-MS), acquired on both high-mass peaks *m/z* 1045 and 1023, were illuminating, however. The two spectra differed significantly from each other: the MS-MS of *m/z* 1045 showed only one intense peak due to the monomer ion at *m/z* 534 ($[M+Na]^+$), whereas *m/z* 1023 yielded a series of fragment ions. This suggested different structures for the Na- and the H-bound high-mass ions. The Na-bound dimer may be interpreted with confidence as a familiar cluster-type ion formed under the ESI and LSI conditions. In contrast, the proton-bound dimer represents a specific strong interaction which is not easy to account for explicitly.

Scheme[1])

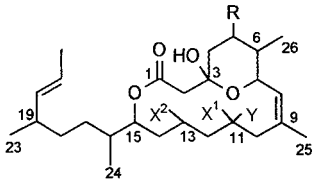

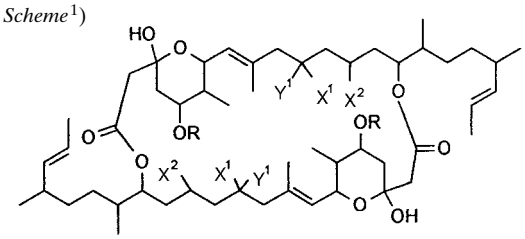

3

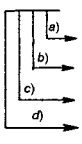

2 R = $OC(O)NH_2$, $X^1 = X^2 = OH$, Y = H
4 R = $OC(O)NH_2$, $X^1 = X^2 = OAc$, Y = H
5 R = $OC(O)NH_2$, $X^1, Y^1 = O$, $X^2 = OH$
6 R = OMe, $X^1 = X^2 = OH$, Y = H
7 R = $OC(O)NH_2$, $X^1–X^2$ = O-C(O)-O, Y = H

a) 1) Excess Ac_2O/pyridine 3:1, r.t., 20 h; 2) TLC (SiO_2); yield 80%.
b) 1) Excess PCC, r.t., 4 h; 2) TLC (SiO_2); yield 60%.
c) 1) Na_2CO_3/MeOH, r.t., 12 h; 2) TLC (SiO_2); yield 60%.
d) 1) 1,1′-Carbonylbis[imidazole] (3 mol-equiv.)/Et_3N, r.t., 48 h; 2) TLC (SiO_2); yield 50%.

The NMR data are thus discussed in relation to the monomeric structures **2** and **4**–**7**. That two O-atoms make part of esterifiable OH groups was shown by diacetylation of **2** to give **4** (*Scheme*). The 300-MHz-^{1}H-NMR data (see *Exper. Part*) helped assigning, in combination with the data below, the position of the two secondary OH groups, although no reliable *J*(H,H) coupling constants could be extracted for either the diacetate **4** or the oxo derivative **5** at this relatively low field. Even at higher field,

[1]) Arbitrary numbering of the backbone; for systematic names, see *Exper. Part.*

600 MHz, proton signals in 1D spectra were largely overlapped which required 2D experiments. Thus, the whole C(4)–C(22)[1]) fragment and methyl branches of **2** were supported by TOCSY and ECOSY data, as summarized in the *Table*. Moreover, HMBC experiments (selected results in the *Table*) allowed us to both extend the sequence from C(4) to C(1) (which was also supported by ROESY maps H_S–C(4) ↔ H_S–C(2) and H_R–C(4) ↔ H_R–C(2)[2])) and to locate the tetrahydro-2*H*-pyran ring[3]). The preferential conformation for leucascandrolide B is displayed by the hand-drawn sketch **2** (*Fig.*, *a*), which approximates the output of molecular-mechanics calculations. A simplified model, with an isopropyl group in place of the side chain of **2**, is shown in the *Figure, b* as the output from semiempirical calculations at the AM1 level. Both models agree with the NMR data of **2** (*Table*), in particular the coupling pattern for the axial protons H_S–C(4)[2]), H–C(5), H–C(6), and H–C(7), as well as the ROESY maps H_R–C(4) ↔ H–C(5), H–C(5) ↔ Me(26), and Me(26) ↔ H–C(7) (*Table*). ROESY maps between H–C(8) and both H–C(6) and Me(26), as well as $J(8,7) = 8.5$, suggested a value of 180° for the dihedral angle H–C(7)–C(8)–H, while the ROESY map H–C(8) ↔ Me(25) supports (*Z*) configuration at the olefinic bond. This, and the correlation C(1) ↔ H–C(15), suggested closure the lactone ring between C(1) and C(15). Additional support for the conformation **2** and the model in the *Figure*, *b*, was given by ROESY maps for, sequentially, the protons drawn inside the macrocycle (H–C(7) ↔ H_R–C(10), H_R–C(10) ↔ H_R–C(12), H_R–C(12) ↔ H–C(13), H–C(13) ↔ H–C(15) and for those drawn outside it (H_S–(10) ↔ H–C(11), H–C(11) ↔ H_S–C(12)). No ROESY correlation maps between these two different groups of protons were found. This conformation with H–C(15) inside the macrocycle imposes the configuration (*S*) at C(15), and thus the position of the side chain, once the configuration (*R*) is arbitrarily attributed to C(3). This has also the consequence of imposing configuration (*S*) at C(11) and (*R*) at C(13), with the OH groups on the same side, outside the macrocycle, thus explaining the facile formation of the cyclic carbonate **7**[4]) from **2**.

It should be noticed that leucascandrolide B (**2**) differs from leucascandrolide A (**1**) by *a*) a smaller (*i.e.* 16- *vs.* 18-membered), not uniformly 1,3-dioxygenated lactone ring, *b*) the lack of the oxazole moiety at the side chain, and *c*) the extensive methyl branching. Thus, leucascandrolide B (**2**) departs from both the sphinxolide [2] and halichondrin [3] types of macrolides, classes to which – apart from the oxazole moiety in the side chain – leucascandrolide A (**1**) may be attributed instead. These notable structural changes in **2** as compared to **1** are accompanied by a markedly different biological behavior. Thus, in contrast to the powerful antifungal and cytotoxic activity

---

[2]) The subscript symbols *R* and *S* stand for *pro-R* and *pro-S*

[3]) Oxo derivative **5**, selectively obtained from **2** by pyridinium chlorochromate (PCC) treatment, showed a *d* at δ(H) 3.55 ppm for OH–C(13) which coupled with H–C(13), besides a *d* at δ(H) 5.57 for OH–C(3) which coupled with 2 H–C(4) (see *Exper. Part*). This supported the tetrahydro-2*H*-pyran ring

[4]) The shifts of the ^{1}H- and ^{13}C-NMR signals at δ(H) 4.96 (*td*) and δ(C) 72.58 (*d*) of **2** to 3.40 and 78.0, respectively, after MeOH/Na_2CO_3 treatment to give **6**, and replacement of δ(C) 156.40 (*s*) of **2** by δ(H) 3.38 (*s*) and δ(C) 56.7 (*q*) for the MeO group of **6**, supported the carbamate functionality of **2** and gave further evidence for the tetrahydro-2*H*-pyran ring. These data also suggested that the change of **2** into **6** in MeOH/Na_2CO_3 occurs *via* a hemiketal-bridge opening followed by carbamic-acid elimination and stereoselective addition of MeOH. In line with this, leucascandrolide B (**2**), on long standing in CD_3OD, underwent partial deuteriation at C(2), as revealed by ^{1}H-NMR spectra.

Table. *NMR Data* (600 MHz) *of Leucascandrolide B* (**2**)[1])[2]). δ in ppm rel. to $SiMe_4$, J in Hz.

	^{1}H-NMR	^{13}C-NMR	^{1}H,^{1}H-ROESY with	Selected ^{13}C,^{1}H-HMBC maps
C(1)		175.02 (*s*)		2*H*−C(2), *H*−C(15)
2 H−C(2)	H_R: 2.59 (*d*, J_{gem} = 13.2)	44.66 (*t*)	H_R−C(4)	
	H_S: 2.70 (*d*, J_{gem} = 13.2)		H_S−C(4)	
C(3)		96.47 (*s*)		2*H*−C(2), 2*H*−C(4)
2 H−C(4)	H_R 2.32 (*dd*, J_{gem} = 11.6, *J*(4*R*,5) = 4.7)	40.85 (*t*)	H−C(5), H_R−C(2)	
	H_S 1.46 (*t*, J_{gem} = *J*(4*S*,5) = 11.6)		H_S−C(2)	
H−C(5)	4.96 (*td*, *J*(5,4*S*) = 11.6, *J*(5,4*R*) = 4.7, *J*(5,6) = 11.0)	72.58 (*d*)	H_R−C(4), Me(26)	
H−C(6)	1.51 (*tq*, *J*(6,5) = 11.0, *J*(6,7) = 10.2, *J*(6,26) = 6.6)	41.52 (*d*)	H−C(8)	
H−C(7)	4.39 (*dd*, *J*(7,6) = 10.2, *J*(7,8) = 8.5)	69.69 (*d*)	H_R−C(10), Me(26)	
H−C(8)	5.11 (br. *d*, *J*(8,7) = 8.5, *J*(8,10*S*) = 2.2, *J*(8,25) = 1.2)	126.77 (*d*)	H−C(6), Me(26)	*H*−C(7), CH_3(25)
C(9)		140.40 (*s*)		
2 H−C(10)	H_R: 2.68 (*dd*, J_{gem} = 14.2, *J*(10*R*,11) = 11.4)	37.44 (*t*)	H−C(7), H−C(13)	
	H_S: 2.39 (br. *dd*, J_{gem} = 14.2, *J*(10*S*,8) = 2.2, *J*(10*S*,11) = 5.2, *J*(10*S*,25) = 1.2, *J*(10*S*,12*S*) small)		Me(25), H−C(11)	
H−C(11)	4.12 (*m*, *J*(11,10*R*) = 11.4, *J*(11,10*S*) = 5.2, *J*(11,12*R*) = 3.0, *J*(11,12*S*) = 2.9)	68.52 (*d*)	H_S−C(10), H_S−C(12)	
2 H−C(12)	H_R: 1.43 (*td*, J_{gem} = 14.5, *J*(12*R*,11) = 3.0, *J*(12*R*,13) = 2.7)	37.12 (*t*)	H−C(13)	
	H_S: 1.83 (*ddd*, J_{gem} = 14.5, *J*(12*S*,13) = 11.6, *J*(12*S*,11) = 2.9, *J*(12*S*,10*S*) small)		H−C(11)	
H−C(13)	4.16 (*tt*, *J*(13,12*S*) = 11.6, *J*(13,12*R*) = 2.7, *J*(13,14*S*) = 10, *J*(13,14*R*) = 2.5)	64.28 (*d*)	H_R−C(10), H−C(15) H_R−C(12)	
2 H−C(14)	H_R: 1.54 (*ddd*, J_{gem} = 14.4, *J*(14*R*,15) = 11.0, *J*(14*R*,13) = 2.5)	40.95 (*t*)		
	H_S: 1.48 (*ddd*, J_{gem} = 14.4, *J*(14*S*,13) = 10.0, *J*(14*S*,15) = 2.5)			
H−C(15)	5.03 (*ddd*, *J*(15,14*R*) = 11.0, *J*(15,14*S*) = 2.5, *J*(15,16) = 4.6)	75.35 (*d*)	H−C(13), Me(24)	CH_3(24), 2*H*−C(17)
H−C(16)	1.56 (*m*, *J*(16,15) = 4.6, *J*(16,24) = 6.9, *J*(16,17a) = 8.0, *J*(16,17b) = 4.5)	36.44 (*d*)		
2 H−C(17)	H_a: 1.08 (*m*, J_{gem} = 12.7, *J*(17a,16) = 8.0, *J*(17a,18a) = 4.5, *J*(17a,18b) = 11.0)	30.71 (*t*)		
	H_b: 1.33 (*m*, J_{gem} = 12.7, *J*(17b,16) = 4.5, *J*(17b,18a) = 11.0, *J*(17b,18b) = 4.5)			
2 H−C(18)	H_a: 1.16 (*m*, J_{gem} = 13.0, *J*(18a,19) = 7.5, *J*(18a,17a) = 4.5, *J*(18a,17b) = 11.0)	34.26 (*t*)		
	H_b: 1.26 (*m*, J_{gem} = 13.0, *J*(18b,19) = 6.0, *J*(18b,17a) = 11.0, *J*(18b,17b) = 4.5)			
H−C(19)	1.97 (*m*, *J*(19,18a) = 7.5, *J*(19,18b) = 6.0, *J*(19,20) = 7.7, *J*(19,23) = 6.6, *J*(19,21) = 1.1)	36.78 (*d*)		
H−C(20)	5.23 (*ddq*, *J*(20,21) = 15.2, *J*(20,19) = 7.7, *J*(20,22) = 1.7)	137.12 (*d*)		CH_3(23), 2*H*−C(18)
H−C(21)	5.34 (*ddq*, *J*(21,20) = 15.2, *J*(21,22) = 6.3, *J*(21,19) = 1.1)	123.16 (*d*)		
Me(22)	1.63 (*dd*, *J*(22,21) = 6.3, *J*(22,20) = 1.7)	17.92 (*q*)		
Me(23)	0.92 (*d*, *J*(23,19) = 6.6)	20.72 (*q*)		
Me(24)	0.89 (*d*, *J*(24,16) = 6.9)	14.80 (*q*)	H−C(15)	
Me(25)	1.67 (*t*, *J*(25,8) = *J*(25,10*S*) = 1.2)	22.16 (*q*)	H−C(8), H_S−C(10)	
Me(26)	0.86 (*d*, *J*(26,6) = 6.6)	13.10 (*q*)	H−C(5), H−C(7), H−C(8)	
CON		156.40 (*s*)		*H*−C(5)

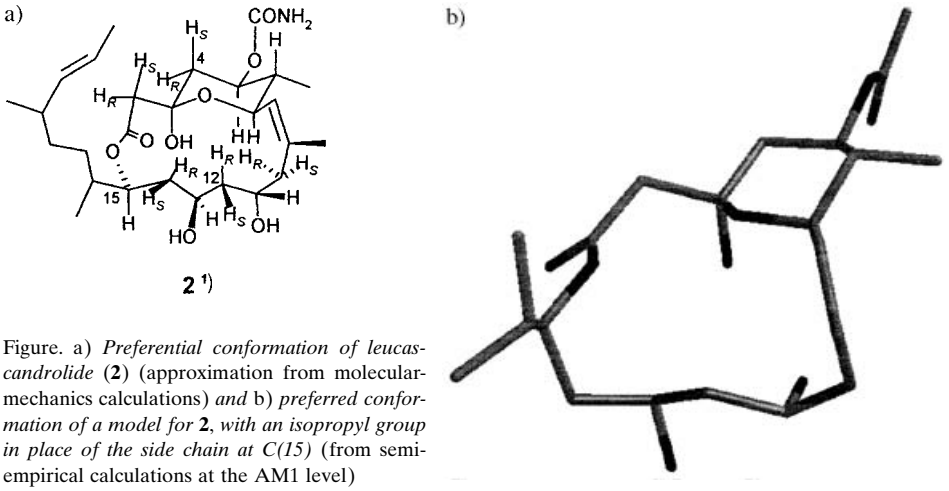

Figure. a) *Preferential conformation of leucascandrolide* (**2**) (approximation from molecular-mechanics calculations) *and* b) *preferred conformation of a model for* **2**, *with an isopropyl group in place of the side chain at C(15)* (from semi-empirical calculations at the AM1 level)

of leucascandrolide A (**1**), leucascandrolide B (**2**) showed only marginal cytotoxicity on tumor cell lines, with an IC_{50} of 5 μg/ml on KB cells and >10 μg/ml on P388 murine leukemia cells and no activity on *Candida albicans.*

It is to be remarked that samples of *L. caveolata* collected in 1994 further north with respect to the 1989 sampling along the northeastern coast of New Caledonia [1] did not contain any trace of either **1** or **2**, suggesting a microbial origin of these products. A mixed assembly of microbes would best explain the profound structural differences in the two macrolides. Isolation of both **1** and **2** in great abundance from the 1989 sampling of *L. caveolata* could be explained by the presence of extensive dead – and thus possibly extensively colonized – portions of the sponge. In this light, these putative microbes appear to be opportunistic rather than symbiotic, explaining why they may be found or not in different sponge samples, and why the structures of both **1** and **2** are so unusual for calcareous sponges.

We thank *S. Gadotti* and *A. Sterni* for technical help with product isolation and *Kratos* MS experiments, *G. Bargibant* and *J.-L. Menou* (ORSTOM, Nouméa) for collection of the sponge as well as *F. Lavelle* (Biology Department, *Rhône Poulenc Rorer*) for the P388 bioassays. Financial support by *MURST*, Roma (*Progetti di Interesse Nazionale*), and *CNR*, Roma (including also the *Progetto Strategico* 96-05073), to Trento, and by *EC Training and Mobility of Researchers – Access to Large-Scale Facilities (EC/CNR* Contract ERB FMGECT95 0061) to Naples, is gratefully acknowledged.

Experimental Part

General. See [1]. Moreover, yields are given on reacted substrate. Prep. TLC: *Merck* silica gel *60* PF_{254}, 2 mm thick plates. Single-stage MS experiments: *Kratos MS-80* mass spectrometer for EI and FAB spectra when indicated; otherwise *Autospec-oa-TOF* (*Micromass*) in the positive-ion mode using different ionization techniques such as matrix-assisted laser desorption (MALDI), electrospray (ESI), and electron ionization (EI). MALDI-MS: in bypass mode with a standard N_2 laser (*LSI V770i*) operating at 330 nm at full energy with 15 shots/s; a 1-μl sample containing 2 pmol of substance was applied directly to the probe using a sat. soln. of dihydroxybenzoic-acid matrix. EI-MS: at 70 eV ionization potential under standard conditions in the mass range *m/z* 50–600. ESI-MS: 10-μl sample aliquots at 20 pmol/μl concentration were introduced through a *Rheodyne* external-loop injector into the ion source at a flow rate set to 10 μl/min with a *Phoenix-20-CU* HPLC pump; as buffer solution, H_2O/MeCN 1:1 containing 0.1% (*v*/*v*) AcOH was applied; spraying was achieved with N_2

nebulizing gas with a probe voltage of 3.6 kV, at a declustering potential (cone voltage) of 40 V and a source temp. of 65°; calibration of the mass scale with multiply-charged ions of horse-heart myoglobin from a separate sample introduction; full-scan MS in continuous data-acquisition mode in the range of *m/z* 300–1500 at a scan rate of 8 s/scan. Selected ions produced by MALDI were further analyzed by high-energy collision induced dissociation (CID) experiments with Ar as collision gas at 800 eV collision potential. Liquid secondary ion (LSI) experiments: *VG-ZAB-T-Four-Sector* (geometry BEBE) mass spectrometer (*Micromass*) with 3-nitrobenzyl alcohol (NBA) as matrix; Cs^+ gun at 30 kV potential; probe accurate mass measurements in the presence of polyethylene glycol as internal standard at 5000 resolution. CID tandem mass spectrometric experiments (MS-MS): only the monoisotopic peak (^{12}C) of the precursor ion was selected; Ar was used as collision gas at a pressure corresponding to 75% attenuation of the precursor-ion beam; product-ion spectra acquired with a 2048 micro-channel photo-diode array detector placed after E_2; angle of the face of the array detector relative to the incoming ion beam 30°, getting a product-ion resolution of *ca.* 1000 (FWHM resolution) with a mass accuracy >0.3 amu; exposure time 0.5 s and mass range from *m/z* 50 amu to the mass of the precursor ion. Data acquisitions and processing: *Opus* software. Molecular-mechanics calculations: 'PCMODEL' program for 'Windows' (V. 1.0, 1993, by *Serena Software*, Bloomington, Indiana). Semiempirical calculations at the AM1 level: 'PC Spartan Plus' program (*Wavefunction*, Irvine, California).

Isolations. Leucascandrolide B (**2**) (72 mg, 0.0003% of freeze-dried-sponge weight, 0.04% of org. extract weight) was obtained from a previous extract [1], by the same methodology (t_R 6.5 min).

Leucascandrolide B (= *(1*R*,5*S*,7*R*,9*S*,13*R*,14*R*,15*R*,11Z)-5-[(*E*)-1,4-Dimethylhept-5-enyl]-1,7,9-trihydroxy-11,14-dimethyl-3-oxo-4,17-dioxabicyclo[11.3.1]heptadec-11-en-15-yl Carbamate*; **2**). $[\alpha]_{589}^{20} = -2$, $[\alpha]_{577}^{20} = +16$ ($c = 0.19$ g/100 ml, $CHCl_3$); $[\alpha]_{589}^{20} = +2$, $[\alpha]_{577}^{20} = +15$ ($c = 0.29$ g/100 ml, EtOH). NMR: *Table.* MS: see text. Moreover, FAB-MS (probe accurate mass measurement; NBA): 534.306343 ± 0.0021 ($C_{27}H_{45}NO_8Na^+$; calc. 534.304288).

Acetylation of **2**. Standard treatment of **2** (6 mg, 0.012 mmol) with excess Ac_2O/dry pyridine 3:1 at r.t. for 20 h, followed by prep. TLC (petroleum ether/AcOEt 2:3), gave 5 mg (80%) of *(1*R*,5*S*,7*R*,9*S*,13*R*,14*R*,15*R*,11Z)-7,9-diacetoxy-5-[(*E*)-1,4-dimethylhept-5-enyl]-1-hydroxy-11,14-dimethyl-3-oxo-4,17-dioxabicyclo-[11.3.1]heptadec-11-en-15-yl carbamate* (**4**). $R_f = 0.7$. ^{1}H-NMR ($CDCl_3$, 299.94 MHz)[1])[2]): 2.53 (*d*, H_R–C(2)); 2.65 (*d*, H_S–C(2)); 2.29 (*dd*, H_R–C(4)); 1.47 (*t*, H_S–C(4)); 5.00 (*td*, H–C(5)); superimposed at 1.55 (*m*, H–C(6)); 4.43 (*t*, H–C(7)); 5.25 (br.*d*, H–C(8)); 2.20 (br. *dd*, H_S–C(10)); 2.81 (br.*t*, H_R–C(10)); 5.13 (*m*, H–C(11) or H–C(13)); 1.50–1.85 (overlapping, *m*, 2 H–C(12), 2 H–C(14)); 5.15 (*m*, H–C(13) or H–C(11)); 5.04 (*m*, H–C(15)); 1.55 (overlapping, *m*, H–C(16)); 1.15, 1.35 (overlapping *m*, 2 H–C(17), 2 H–C(18)); 1.97 (*m*, H–C(19)); 5.23 (*ddq*, H–C(20)); 5.34 (*ddq*, H–C(21)); 1.63 (br.*d*, Me(22)); 0.92 (*d*, Me(23)); 0.85 (*d*, Me(24)); 1.74 (br. *s*, Me(25)); 0.84 (*d*, Me(26)); 2.02, 2.05 (2*s*, MeCO). ^{13}C-NMR ($CDCl_3$, 75.43 MHz)[1]): 170.5 (*s*, C(1)); 45.6 (*t*, C(2)); 96.8 (*s*, C(3)); 41.0 (*t*, C(4)); 72.8 (*d*, C(5)); 41.3 (*d*, C(6)); 69.6 (*d*, C(7)); 128.3 (*d*, C(8)); 138.8 (*s*, C(9)); 36.0 (*t*, C(10)); 68.5 (*d*, C(11) or C(13)); 35.3 (*t*, C(12)); 67.6 (*d*, C(13) or C(11)); 37.8 (*t*, C(14)); 73.6 (*d*, C(15)); 38.2 (*d*, C(16)); 30.2 (*t*, C(17)); 34.3 (*t*, C(18)); 36.8 (*d*, C(19)); 137.3 (*d*, C(20)); 123.0 (*d*, C(21)); 17.9 (*q*, C(22)); 20.7 (*q*, C(23)); 14.5 (*q*, C(24)); 22.3 (*q*, C(25)); 13.1 (*q*, C(26)); 156.2 (*s*, CON); 171.0, 171.2 (2*s*, Me*C*O); 21.2, 21.3 (*q*, *Me*CO). EI-MS (*Kratos*): 534 (1, $[M - H_2NCOOH]^{+\cdot}$), 475 (2, $[M - 2AcOH]^{+\cdot}$), 43 (100). FAB-MS (NBA; *Kratos*): 620, 619, 618 ($[M + Na]^+$).

Oxidation of **2**. Standard treatment of **2** (5 mg, 0.010 mmol) with pyridinium chlorochromate in excess at r.t. for 4 h, followed by prep. TLC (petroleum ether/AcOEt 2:3), gave 3 mg (60%) of *(1*R*,5*S*,7*S*,13*R*,14*R*,15*R*,11Z)-[(*E*)-1,4-dimethylhept-5-enyl]-1,7-dihydroxy-11,14-dimethyl-3,9-dioxo-4,17-dioxabicyclo[11.3.1]-heptadec-11-en-15-yl carbamate* (**5**). R_f 0.6. ^{1}H-NMR ($CDCl_3$, 299.94 MHz)[1])[2]): 2.60 (*d*, H_R–C(2)); 2.72 (*d*, H_S–C(2)); 5.57 (*d*, OH–C(3)); 2.33 (*dd*, H_R–C(4)); 1.49 (*td*, H_S–C(4)); 4.97 (*td*, H–C(5)); 1.5 (overlapping, *m*, H–C(6)); 4.34 (*dd*, H–C(7)); 5.40 (br.*d*, H–C(8)); 2.78 (br.*d*, H_S–C(10)); 3.62 (*d*, H_R–C(10)); 2.70 (*dd*, H_R–C(12)); 2.30 (*dd*, H_S–C(12)); 4.21 (*m*, H–C(13)); 3.55 (*d*, OH–C(13)); 1.55–1.75 (*m*, 2 H–C(14)); 5.08 (*ddd*, H–C(15)); 1.6 (superimposed, 2*m*, H–C(16)); 1.05, 1.35 (superimposed *m*, 2 H–C(17), 2 H–C(18)); 1.97 (*m*, H–C(19)); 5.22 (*ddq*, H–C(20)); 5.34 (*ddq*, H–C(21)); 1.63 (*dd*, Me(22)); 0.92 (*d*, Me(23)); 0.89 (*d*, Me(24)); 1.68 (br. *s*, Me(25)); 0.89 (*d*, Me(26)). ^{13}C-NMR ($CDCl_3$, 75.43 MHz)[1]): 174.1 (*s*, C(1)); 44.3 (*t*, C(2)); 96.8 (*s*, C(3)); 40.9 (*t*, C(4)); 72.4 (*d*, C(5)); 41.4 (*d*, C(6)); 70.1 (*d*, C(7)); 129.0 (*d*, C(8)); 136.9 (*s*, C(9)); 47.5 (*t*, C(10)); 209.9 (*s*, C(11)); 47.5 (*t*, C(12)); 65.7 (*d*, C(13)); 39.7 (*t*, C(14)); 76.1 (*d*, C(15)); 37.8 (*d*, C(16) or C(19)); 30.6 (*t*, C(17)); 34.3 (*t*, C(18)); 36.8 (*d*, C(19) or C(16)); 137.1 (*d*, C(20)); 123.2 (*d*, C(21)); 18.0 (*q*, C(22)); 20.8 (*q*, C(23)); 14.6 (*q*, C(24)); 22.8 (*q*, C(25)); 13.0 (*q*, C(26)); 156.1 (*s*, CON). EI-MS (*Kratos*): 430 (28, $[M - H_2NCOOH - H_2O]^{+\cdot}$), 69 (100). FAB-MS (*Kratos*; NBA): 532 ($[M + Na]^+$).

Alkaline Methanolysis of **2**. Treatment of **2** (5 mg, 0.010 mmol) with Na_2CO_3 (2 mg) in MeOH (1 ml) by stirring at r.t. for 12 h, followed by prep. TLC (petroleum ether/AcOEt 2:3), gave 3 mg (60%) of *(1*R*,5*S*,7*R*,9*S*,13*R*,14*S*,15*R*,11Z)-5-[(*E*)-1,4-dimethylhept-5-enyl]-1,7,9-trihydroxy-15-methoxy-11,14-dimethyl-4,17-dioxabicyclo[11.3.1]heptadec-11-en-3-one* (**6**). ^{1}H-NMR ($CDCl_3$, 299.94 MHz[1])[2]): 2.61 (*d*, H_R–C(2)); 2.74 (*d*, H_S–C(2)); 2.32 (*dd*, H_R–C(4)); 1.29 (*t*, H_S–C(4)); 3.40 (*td*, H–C(5)); 1.44 (superimposed, *m*, H–C(6), H_R–C(12)); 4.31 (*dd*, H–C(7)); 5.13 (br.*d*, H–C(8)); 2.40 (br. *dd*, H_S–C(10)); 2.69 (*dd*, H_R–C(10)); 4.13 (*m*, H–C(11)); 1.84 (*ddd*, H_S–C(12)); 4.17 (*m*, H–C(13)); 1.40–1.60 (superimposed, *m*, 2 H–C(14)); 5.04 (*m*, H–C(15)); 1.5 (superimposed, *m*, H–C(16)); 1.05–1.35 (superimposed, *m*, 2 H–C(17), 2 H–C(18)); 1.98 (*m*, H–C(19)); 5.24 (*ddq*, H–C(20)); 5.36 (*ddq*, H–C(21)); 1.64 (br.*d*, Me(22)); 0.93 (*d*, Me(23)); 0.90 (*d*, Me(24)); 1.68 (br. *s*, Me(25)); 0.89 (*d*, Me(26)); 3.38 (*s*, MeO). ^{13}C-NMR ($CDCl_3$, 75.43 MHz[1]): 175.3 (*s*, C(1)); 45.0 (*t*, C(2)); 96.7 (*s*, C(3)); 39.7 (*t*, C(4)); 78.0 (*d*, C(5)); 42.5 (*d*, C(6)); 69.9 (*d*, C(7)); 127.2 (*d*, C(8)); 139.9 (*s*, C(9)); 37.5 (*t*, C(10)); 68.6 (*d*, C(11)); 37.1 (*t*, C(12)); 64.3 (*d*, C(13)); 41.0 (*t*, C(14)); 75.4 (*d*, C(15)); 36.6 (*d*, C(16)); 30.7 (*t*, C(17)); 34.3 (*t*, C(18)); 36.8 (*d*, C(19)); 137.1 (*d*, C(20)); 123.2 (*d*, C(21)); 17.9 (*q*, C(22)); 20.7 (*q*, C(23)); 14.8 (*q*, C(24)); 22.1 (*q*, C(25)); 13.2 (*q*, C(26)); 56.7 (*q*, MeO). EI-MS (*Kratos*): 434 (5), 433 (7), 432 (5, $[M - MeOH - H_2O]^{+\cdot}$), 69 (100). HR-EI-MS (*Kratos*): 432.28660 ± 0.01 ($C_{26}H_{40}O_5^{+\cdot}$, $[M - MeOH - H_2O]^{+\cdot}$; calc. 432.28757). FAB-MS (NBA; *Kratos*): 508, 507, 506, 505 ($[M + Na]^+$).

Treatment of **2** *with 1,1′-Carbonylbis[1*H*-imidazole]/Et$_3$N.* Compound **2** (12 mg, 0.023 mmol) was treated with 3 mol equiv. of carbonylbis[1*H*-imidazole] (7 mg) in dry Et_3N (1 ml) at r.t. for 48 h. The mixture was then subjected to prep. TLC (petroleum ether/AcOEt 3:7) to give 2 mg (50%) of *(1*R*,5*S*,7*S*,9*S*,13*R*,14*R*,15*R*,11Z)-7,9-(carbonyldioxy)-5-[(*E*)-1,4-dimethylhept-5-enyl]-1-hydroxy-11,14-dimethyl-3-oxo-4,17-dioxabicyclo[11.3.1]heptadec-11-en-15-yl carbamate* (**7**; R_f = 0.7) besides 8 mg of unreacted **2** (R_f 0.4). Data of **7**: ^{1}H-NMR ($CDCl_3$, 600 MHz[1])[2]): 2.58 (*d*, J_{gem} = 13.5, H_R–C(2)); 2.67 (*d*, J_{gem} = 13.2, H_S–C(2)); 5.62 (*d*, J(3,4*S*) = 2.0, OH–C(3)); 2.30 (*dd*, J_{gem} = 11.5, J(4*R*,5) = 4.5, H_R–C(4)); 1.48 (*td*, $J_{gem} = J$(4*S*,5) = 11.5, J(*4*S,3) = 2.0, H_S–C(4)); 4.99 (*td*, J(5,4*S*) = 11.5, J(5,4*R*) = 4.5, J(5,6) = 10.5, H–C(5)); 1.53 (*tq*, J(6,5) = J(6,7) = 10.5, J(6,26) = 6.5, H–C(6)); 4.30 (*dd*, J(7,6) = 10.5, J(7,8) = 7.8, J(7,25) = small, H–C(7)); 5.28 (br.*d*, J(8,7) = 7.8, J(8,10*S*) = J(8,25) = 1.2, H–C(8)); 2.61 (br. *dd*, J_{gem} = 14.0, J(10*S*,8) = 1.2, J(10*S*,11) = 5.5, J(10*S*,25) = J(10*S*,12*S*) = small, H_S–C(10)); 2.73 (*dd*, J_{gem} = 14.0, J(10*R*,11) = 11.0, H_R–C(10)); 4.80 (*m*, J(11,10*R*) = 11.0, J(11,10*S*) = J(11,12*S*) = 5.5, J(11,12*R*) = 2.2, H–C(11)); 1.76 (*dt*, J_{gem} = 14.5, J(12*R*,11) = 2.2, J(12*R*,13) = 3.0, H_R–C(12)); 1.95 (*ddd*, J_{gem} = 14.5, J(12*S*,13) = 11.5, J(12*S*,11) = 5.5, J(12*S*,10*S*) = small, H_S–C(12)); 4.59 (*ddt*, J(13,12*S*) = 11.5, J(13,14*S*) = 9, J(13,12*R*) = J(13,14*R*) = 3, H–C(13)); superimposed at 1.78 (*m*, 2 H–C(14)); 5.46 (*m*, H–C(15)); 1.57 (*m*, H–C(16)); 1.06, 1.34 (2*m*, 2 H–C(17)); 1.20, 1.30 (2*m*, 2 H–C(18)); 1.98 (*m*, J(19,20) = 7.5, J(19,23) = 6.6, J(19,21) = 1.0, H–C(19)); 5.24(*ddq*, J(20,21) = 15.2, J(20,19) = 7.5, J(20,22) = 1.2, H–C(20)); 5.36 (*ddq*, J(21,20) = 15.2, J(21,22) = 6.3, J(21,19) = 1.0, H–C(21)); 1.64 (*dd*, J(22,21) = 6.3, J(22,20) = 1.2, Me(22)); 0.94 (*d*, J(23,19) = 6.6, Me(23)); 0.91 (*d*, J(24,16) = 6.9, Me(24)); 1.72 (br.*s*, J(25,8) = 1.2, J(25,7) = J(25,10*S*) = small, Me(25)); 0.89 (*d*, J(26,6) = 6.5, Me(26)). ^{13}C-NMR ($CDCl_3$, 75.43 MHz): 172.4 (*s*, C(1)); 44.1 (*t*, C(2)); 96.9 (*s*, C(3)); 41.3 (*t*, C(4)); 72.3 (*d*, C(5)); 41.7 (*d*, C(6)); 69.6 (*d*, C(7)); 129.9 (*d*, C(8)); 137.3 (*s*, C(9)); 35.0 (*t*, C(10)); 74.9 (*d*, C(11)); 28.5 (*t*, C(12)); 71.3 (*d*, C(13)); 39.0 (*t*, C(14)); 73.6 (*d*, C(15)); 36.9 (*d*, C(16)); 30.6 (*t*, C(17)); 34.5 (*t*, C(18)); 36.9 (*d*, C(19)); 137.2 (*d*, C(20)); 123.2 (*d*, C(21)); 18.0 (*q*, C(22)); 20.8 (*q*, C(23)); 14.3 (*q*, C(24)); 21.9 (*q*, C(25)); 13.2 (*q*, C(26)); 156.0 (*s*, CON); 148.8 (*s*, OCOO). Selected HMBC maps: C(1) ↔ H_R–C(2), H_S–C(2) and *H*–C(15); C(3) ↔ O*H*–C(3), *H*–C(7), H_R–C(2), H_S–C(2), H_R–C(4) and H_S–C(4); C(9) ↔ *H*–C(7), H_R–C(10), H_S–C(10) and CH_3(25); C(15) ↔ CH_3(24) and 2*H*–C(17); C(20) ↔ CH_3(23) and 2*H*–C(18); CON ↔ *H*–C(5); OCOO ↔ *H*–C(11) and H_S–C(14). EI-MS (*Kratos*): 476 (1.1, $[M - H_2NCOOH]^{+\cdot}$), 458 (2, $[M - H_2NCOOH - H_2O]^{+\cdot}$), 44 (100). HR-EI-MS (*Kratos*): 476.27728 ± 0.005 ($C_{27}H_{40}O_7^{+\cdot}$, $[M - H_2NCOOH]^{+\cdot}$; calc. 476.27740), 458.26575 ± 0.005 ($C_{27}H_{38}O_6^{+\cdot}$, $[M - H_2NCOOH - H_2O]^{+\cdot}$; calc. 458.26683).

REFERENCES

[1] M. D'Ambrosio, A. Guerriero, C. Debitus, F. Pietra, *Helv. Chim. Acta* **1996**, *79*, 51.
[2] G. Guella, I. Mancini, G. Chiasera, F. Pietra, *Helv. Chim. Acta* **1989**, *72*, 237.
[3] G. R. Pettit, C. L. Herald, M. R. Boyd, J. E. Leet, C. Dufresne, D. L. Doubeck, J. M. Schmidt, R. L. Cerny, J. N. A. Hooper, K. C. Rützler, *J. Med. Chem.* **1991**, *34*, 3339.

Received December 22, 1998